Hairy Slices: Evaluating the Perceptual Effectiveness of Cutting Plane Glyphs for 3D Vector Fields

Andrew H. Stevens, Thomas Butkiewicz, and Colin Ware

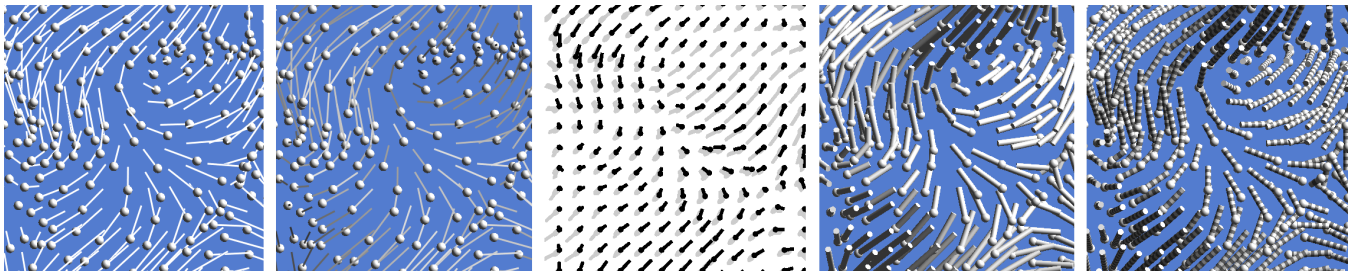

Fig. 1. The five glyph techniques evaluated in this study: plain lines, illuminated lines, shadowed lines, plain tubes, and ringed tubes.

Abstract— Three-dimensional vector fields are common datasets throughout the sciences. Visualizing these fields is inherently difficult due to issues such as visual clutter and self-occlusion. Cutting planes are often used to overcome these issues by presenting more manageable slices of data. The existing literature provides many techniques for visualizing the flow through these cutting planes; however, there is a lack of empirical studies focused on the underlying perceptual cues that make popular techniques successful. This paper presents a quantitative human factors study that evaluates static monoscopic depth and orientation cues in the context of cutting plane glyph designs for exploring and analyzing 3D flow fields. The goal of the study was to ascertain the relative effectiveness of various techniques for portraying the direction of flow through a cutting plane at a given point, and to identify the visual cues and combinations of cues involved, and how they contribute to accurate performance. It was found that increasing the dimensionality of line-based glyphs into tubular structures enhances their ability to convey orientation through shading, and that increasing their diameter intensifies this effect. These tube-based glyphs were also less sensitive to visual clutter issues at higher densities. Adding shadows to lines was also found to increase perception of flow direction. Implications of the experimental results are discussed and extrapolated into a number of guidelines for designing more perceptually effective glyphs for 3D vector field visualizations.

Index Terms— Flow visualization, 3D vector fields, Cutting planes, Glyphs, Perception, Evaluation, Human factors

1 Introduction

Flow visualization, a category of vector field visualization, deals primarily with velocities (speed and direction), and focuses on visually communicating features of interest such as critical points (saddles, sinks, and sources), maxima and minima, and specific flow patterns. 3D flow visualization is a natural extension of the 2D case, but is inherently more challenging, due to issues such as self-occlusion and visual clutter. Beyond just flow, these 3D vector fields are encountered in many scientific disciplines, where they represent everything from magnetic fields to stress and strain in materials.

There are four families of 3D vector field visualizations: geometric or integral flow approaches, which are based on tracing advected particles; texture-based flow, which uses dense sets of seeds (often a white-noise image) that are "smeared" by the flow field; feature flow, which uses computations on a global scale to identify, extract, and visualize the salient features in a flow field; and flow glyphs, which are direct visualizations of the data using objects that encode local information (location, direction, and magnitude).

- *Andrew H. Stevens is with The Center for Coastal and Ocean Mapping at The University of New Hampshire. E-mail: astevens@ccom.unh.edu.*
- *Thomas Butkiewicz is with The Center for Coastal and Ocean Mapping at The University of New Hampshire. E-mail: tbutkiewicz@ccom.unh.edu.*
- *Colin Ware is with The Center for Coastal and Ocean Mapping at The University of New Hampshire. E-mail: cware@ccom.unh.edu.*

Cutting planes are often used to interactively reduce the dimensionality of 3D vector fields into more cognitively manageable 2D slices. Applying 3D glyphs to these cutting planes is a common choice, as they can present an additional dimension of information as opposed to 2D techniques such as color mapping and texturing.

Many glyph techniques have been proposed and studied by researchers, and a number of effective designs have been identified [1]. However, there is a lack of empirical studies explicitly examining the relative effectiveness of the different visual elements that comprise these popular glyph designs; most related studies are task-based, and do not explicitly address perceptual effectiveness. Indeed, an NSF report on visualization research challenges noted there were "disproportionately few quantitative studies comparing visualization techniques" [2]. This study directly addresses this need by contributing a controlled perceptual evaluation of the most popular glyph techniques in 3D vector field visualization.

It is critical to understand and identify the particular visual cues that make visualization techniques successful, as this provides guidelines that can inform future design decisions. This study seeks to determine the principal cues involved and how they contribute to the effectiveness of glyphs on cutting planes. Furthermore, it investigates which combinations of these cues reinforce one another, and which combinations have the potential to clash and undermine one another.

Specifically, this paper presents an experiment that tests the perceptual effectiveness of some of the most popular glyph techniques from the literature for their ability to communicate flow direction through a cutting plane. The results of the experiment are discussed, and the significant principal cues and interactions between them are identified. These findings are further extrapolated into a series of

guidelines for effective design of glyph-based 3D vector field visualizations.

2 Related Work

Three-dimensional vector field visualization may superficially appear to be a trivial extension of the 2D case to an extra dimension, but it presents many formidable visualization challenges:

The primary limitation of glyph-based (and other) approaches is self-occlusion, where glyphs closer in depth to the viewer obstruct the view of other glyphs positioned behind them [3]. Similarly, these approaches can also suffer from extreme visual clutter/complexity as seeding densities increase. When there is too much information for the visual system to deal with effectively, it can lead to an obfuscation of global and local patterns, hindering the tasks they are supposed to support. These issues become immediately apparent when using popular software packages such as MATLAB's quiver3 [4] tool, which render vector fields as 3D grids of arrows.

Though there have been efforts to mitigate these particular challenges for 3D glyph-based approaches [5][6], the overwhelming response by researchers has been to develop alternative visualization metaphors and to more intelligently sample data to reduce visual density while retaining the communicative power of the visualization. Laramee et al. [7] describe and implement a variety of these approaches, including geometric streamtubes and texture-based techniques, apply them to slices through CFD flow visualizations, and provide details on their relative strengths and weaknesses.

This paper reflects a different approach: seeking to understand the strength of the various visual cues used in each visualization technique to determine not only *why* particular techniques are effective, but to identify sets of compatible visual cues that can be combined to produce demonstrably better visualizations.

2.1 3D Flow Visualization

Solutions presented in the literature vary widely, with most approaches being extensions of the four most common families of 3D flow visualization methods: flow glyphs, geometric flow, texture flow, and feature flow [3] [7].

Flow glyphs convey local information about the vector field using geometric objects whose substructure is tied directly to the data itself. For example, an arrow with a stem length representing vector magnitude, and an orientation indicating flow direction.

Geometric flow encompasses various integral methods such as *streamlines*, which trace the path of a particle as it advects within a steady flow field; *pathlines*, the streamline analog within unsteady flow fields; and *streamtubes*, a three-dimensional extension of streamlines for 3D flow fields. McLoughlin et al. [8] provide a thorough survey on this family of flow visualizations.

Texture flow is the use of texture-based methods to indicate flow properties, as in the line integral convolution (LIC) technique introduced by Cabral and Leedom [9]. This algorithm advects pixels from generated white noise images through a vector field, "smearing" the noise image and resulting in a texture depicting the flow field, which densely covers the entire region of interest. While LIC methods applied to 3D scenarios are most often used to show flow on surface boundaries [7], the method has also been extended by Interrante and Grosch to be compatible with 3D volumes [10].

Lastly, there is feature-based or topological flow, which attempts to computationally extract and visualize the most salient structures of interest, such as critical points and vortices.

For a detailed exposition on the many solutions presented in the literature, Post et al. [11] provide a useful survey and categorization of the field, along with its challenges and a brief discussion on applying geometric objects to 2D slices, while Ware [12] specifically addresses the perceptual components and common tasks involved in visualizing 2D vector fields for flow.

2.2 Cutting Planes

Cutting planes are tools used to reduce the visual dimensionality of 3D datasets to more manageable 2D slices, which ameliorates many of the issues inherent in volumetric 3D visualizations, such as self-occlusion. Cutting planes are widely implemented in scientific visualization systems [13][14][15], modern open-source visualization toolkits [16], and turnkey software for industry [4][17]. There have even been educational systems designed to train students in their use and improve performance while employing them as a visualization tool [18].

Cutting planes are used in many different ways. They are sometimes used as clipping planes to view structures enclosed within other volumes [7][19], or as seeding planes for geometric visualizations like streamlines and streamtubes [7][13][20]. Studies have examined the use of physically interactive cutting planes, like Meyer and Globus' study [21] on cutting plane use in virtual reality and Hinckley's [22] use of physical props to interactively orient a cutting plane through a model of the brain. These studies emphasize the value of interactively sweeping the cutting plane through the data field to reveal patterns and structure. Often, cutting planes are color-mapped to show 2D scalar data like temperature and magnitude [20][21][23] or used as higher-dimension visual displays that can leverage the effectiveness of 2D visualization methods.

Creating a strong flow visualization on cutting planes is similar to the problem of 2D flow visualization, which has seen some important recent contributions. Laidlaw et al. [24] lay solid quantitative groundwork for assessing the relative merits of commonly used 2D flow methods via empirical task-based evaluation. Liu et al. [25] extend this work to include color mapping and a sophisticated study and analysis design, though with limited evaluation of glyph styles.

There are many techniques for visualizing 3D vectors through a cutting plane. Konrad-Verse et al. [26] present a deformable cutting plane for surgery planning. Modiano [23] and Schulz et al. [20] place scalar color-mapped cutting planes in series, while Fuhrmann's dashtubes [27] make use of an animated, partially transparent texture applied on streamtubes to strongly disambiguate flow direction and lessen occlusion. However, most techniques employ some form of direct or integral visualization using a glyph or other geometry.

2.3 Glyphs and Integral Geometries for Flow Vis

Geometric representation of local flow information is often achieved using fields of glyphs, which individually present the flow data at their immediate locations. Identifying and understanding global patterns and features typically relies on integral geometric techniques. Munzner [3] gives a good overview of the various types of geometries used for 3D flow visualizations, summarized here.

The most common flow glyphs by far are arrows, as encountered in MATLAB's quiver3 function or Wittenbrink's work on visualizing uncertainty with 3D glyphs [28]. Laramee et al. [7] also include techniques in their CFD visualization design study that directly visualize arrows and streamlets (short, tubular glyphs).

Integral geometric structures often involve either simple streamlines, or perceptually superior illuminated streamlines [29], which incorporate a shading model. 3D extensions of streamlines, streamtubes and threads, have been the subject of a number of design studies [7][30][31]. There are numerous other variants, e.g. streamribbons [32] to highlight rotation and torsion. When used with cutting planes, the slices typically serve as a seeding plane for these approaches.

Borgo et al. [1] provide a survey of the wide-ranging uses of glyphs, and a design framework by which to compose glyphs. They highlight the importance of simplicity and symmetry in 3D glyph design, and underscore the need to facilitate depth perception for 3D visualizations, chiefly by careful glyph design and illustrative techniques such as halos and depth cueing. Lie et al. [33] also studied glyphs for visualizing 3D data, and while they make the important observation that 3D glyphs are best suited to data that naturally lends

itself to a 3D representation, their study focuses on 2D billboarded superellipses and lacks a formal user study.

2.4 Visual Cues for Glyph Perception

Many researchers have sought to increase visual clarity by proposing techniques that add or reinforce perceptual cues. (E.g. Chen et al.'s framework [34] for 3D vector field visualization, and Brambilla et al.'s survey [35] of flow visualization).

However, a majority of previous work lacks accompanying user studies that examine what perceptual or task-based gains have been made through new techniques. There are few empirical studies in the literature concerned specifically with 3D glyphs, and most focus on representative task performance, not perceptual effectiveness.

Theories of space perception are based on cues that help build our perception of orientation on the plane orthogonal to the line of sight. When combined with 'depth cues', they contribute to our understanding of the layout and orientation of objects in depth [12]. In the following sections, we summarize the perceptual cues that are most relevant to glyph techniques.

2.4.1 2D Orientation and Direction

Two-dimensional vector representations can be conceptualized as a combination of magnitude and direction with respect to orientation.

Magnitude is often color-coded, but can also be represented by glyph length and/or size.

Direction is indicated by adding asymmetry to a path, the perception of which is tied to neural structures known as end-stopped cells. Arrows are a classic way of indicating direction, but more perceptually effective structures exist (e.g. streaklets and streamlets) that can elicit a stronger response out of the end-stopped cells. Arrows also contribute visual noise via the contours of the arrowheads themselves, the directions of which do not correspond to the underlying flow data.

For 2D flow, orientation is best conveyed with contours or strong directional glyphs that are tangential to the flow.

2.4.2 Depth Cues

Depth cues arguably play the most important role in a 3D flow visualization. We rely on them to help us make spatial distinctions and judgements about objects in our world, and they come in a variety of forms.

Occlusion is not just an annoyance for 3D visualization researchers; it acts as an indispensable cue for distinguishing the relative depths of objects. When one object occludes another, we understand the occluding object to be closer than the occluded object, but we do not have any extra information to determine the distance between them.

Shading-based cues are also of key import to depth perception. Shape-from-shading is the cue that helps us to understand the contours and ridges of 3D surfaces through the shading and texture applied to it. In particular, regularly structured linear surface textures such as simple grids have been found to be helpful in the perception of surface shape.

Cast shadows can also serve as a strong cue, when used correctly. They mainly provide information about the height of an object, but can also give an indirect depth cue by conveying the position of an object within the environment relative to a surface and light source. Similar to shape-from-shading cues, cast shadows are also effective when not realistically rendered. As visual scenes become more complex, the ability to tie shadows to the objects that cast them diminishes, and the cue quickly goes from useful to useless or, worse, a hindrance to understanding the visualization.

Stereoscopic depth cues stem from small differences between the image received by the right eye and that received by the left eye. Though often thought of as "the" 3D depth cue, many other depth cues exist, and experiments have shown that stereoscopic depth is often not the most useful cue for depth perception. Nonetheless, its prominent role in successful 3D flow visualizations has been reinforced by a number of recent quantitative studies [36][37][38].

Another depth cue that has been the subject of recent empirical studies is structure-from-motion. The two main flavors of SfM are kinetic depth, the phenomenon of being able to understand the 3D shape of a rotating bent wire structure solely by viewing its projection on a screen, and motion parallax, where objects closer to us appear to move more quickly than those closer to the horizon when we move laterally. Like stereoscopic depth, SfM has emerged as an important cue for depth perception in controlled evaluations [36][37].

2.4.3 Texture

Texture is an important component of glyph design that can encode additional information or reinforce existing cues. To quote directly, "even if we texture all objects in exactly the same way, this can help us perceive the orientation, shape, and spatial layout of a surface." In fact, textures can be conceptualized as dense fields of glyphs, mapping certain properties of the object to which they are applied.

The human visual system is particularly sensitive to high-contrast grating-type patterns. Textures that employ patterns over certain orientations and spatial frequencies elicit particularly strong responses, as do the boundaries between regions of textures with different orientations.

2.5 Choice of Task

Past studies [24][25][37][39] have concentrated on measuring performance for a wide variety of tasks. They evaluate visualizations in the context of tasks such as estimating advection trajectories, identifying important patterns in the flow structure, and perceiving magnitude, vorticity, turbulence, and other features of a flow field. However, Ware's evaluation [36] of 3D contour orientation is the only qualitative study that focuses specifically on the perceptual performance of these visualization techniques, and it would be beneficial to have more studies that tie perceptual theory to visualization performance.

Ware [36] and Forsberg et al. [37] obtained conflicting results when comparing line-based flow visualization techniques to tube-based techniques. While Ware found that tube-based rendering techniques had a significant advantage over those that are line-based, Forsberg et al. did not observe the same difference, and even found line-based techniques to be better in some circumstances and preferred by the majority of users. It is hard to identify the precise cause of this disagreement, because the experimental designs differed on key aspects. Ware evaluated lit lines along with shaded and ring-textured tubes on a high-resolution display, while Forsberg et al. compared unlit but colored lines along with larger shaded tubes augmented with auxiliary directional glyphs, a dense direction-encoded texture, and halos to help disambiguate the occluding tubes displayed on a standard-resolution monitor. An interesting result from Ware's study is that tube-based visualizations performed remarkably well even under monoscopic conditions. These differences provided the motivation for the experiment described in this paper, which is an objective comparison to differentiate relative perceptual strengths and weaknesses between these two techniques.

Of the set of representative tasks, we restrict ours to a strongly spatial task that supports our objective of perceptual evaluation. Judging the three-dimensional direction of flow at an arbitrary point on a plane is one of the most basic and fundamental tasks in understanding a flow field, and serves as an ideal platform for continuing to piece together the perceptual framework of 3D flow visualization.

Despite the increasing availability of high-quality consumer 3D displays, they still have not become a commonplace item in visualization workstations. In light of this, and because of the numerous studies already confirming the usefulness of stereoscopy in 3D visualization perception, we chose to limit our study to a single monoscopic viewing condition. This also allows us to expand our experiment to cover additional glyph designs, which is the primary focus of this evaluation.

3 EXPERIMENT

The primary purpose of this study was to understand how different static, monoscopic rendering techniques help with the perception of 3D orientation in order to establish perceptually-grounded guidelines for designing an effective cutting plane.

It is hypothesized that those glyph designs which incorporate the most depth and orientation cues will be the most successful for estimating 3D flow direction, such as the plain and ringed tubes. It is further hypothesized that the depth cues provided by cylinders will significantly set apart the tube-based renderings from the others in terms of orientation perception performance.

We created an apparatus combining a high-resolution display to display the renderings in the finest detail discernible to the human eye and an electromagnetic orientation tracking system to accurately and precisely record perceived glyph orientations. The experimental method was meticulously designed to control as many sources of error as possible.

3.1 Apparatus and Display

The experimental apparatus was constructed using a high-definition digital monitor to display the stimuli and a three-dimensional orientation tracking system to record subject responses. These elements were respectively inset and mounted to a rigid piece of black foamboard in order to provide the subject with a clean and distraction-free interface, shown in Figure 2.

Fig. 2. The experimental apparatus, consisting of a 25cm diagonal high-resolution "Retina" display and an electromagnetically tracked hand-held probe for inputting perceived orientation.

An LG LP097QX1 9.7" 60Hz display panel was used due to its high pixel density relative to its size; the 2048 x 1536 pixel across its 197.1mm x 147.8mm screen yields a pixel size of approximately 0.096mm. With subjects seated approximately 57cm from the display, each pixel subtends a visual angle of 34.7 arc seconds, providing about 104 pixels per degree of visual angle. This approximates the size of foveal receptors in the eye [40], allowing for an optimal display resolution congruent with that of the human visual system as well as the finest resolvable non-stereoscopic point and grating acuities (approximately 60 seconds of arc) [12].

3.2 Orientation Tracking

Participants input their perceived orientation using a Polhemus 3Space Isotrak II electromagnetic orientation tracker attached to a physical hand-held probe (shown in Figure 3). The system collects orientation data at 60Hz, with a resolution of 0.1˚, and a root mean square error of 0.75˚.

The electromagnetic tracker was attached to the tip of a physical probe, consisting of a 2cm x 2cm x 10cm block of rigid foam, textured with a 1cm² grid pattern. This physical shape and texture combination was designed to provide strong linear perspective depth cues, while being visually dissimilar to any of the rendering methods, thereby eliminating the possibility of the experimental task devolving into one-to-one matching between physical probe and on-screen stimuli.

The tracker system was physically calibrated to the experimental setup, and electromagnetic field interference from the display and other nearby equipment was found to contribute no more than approximately 1˚ error on average.

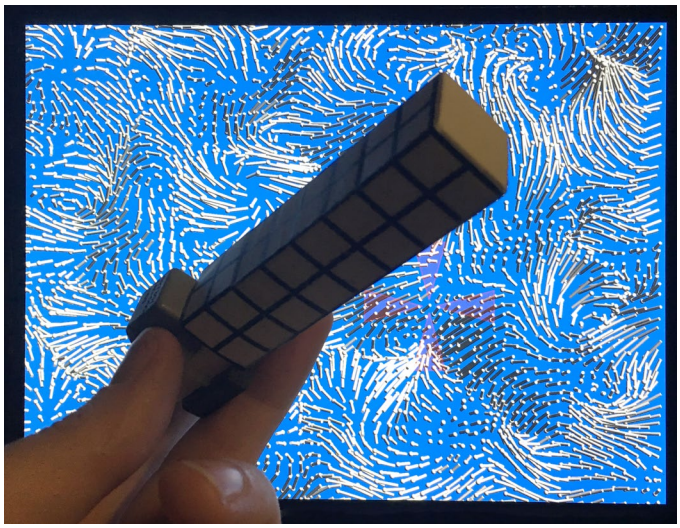

Fig. 3. The physical hand-held probe device that subjects used to indicate perceived orientation.

3.3 Task

Subjects were first screened with a vision test to verify at least 20/20 binocular visual acuity prior to participation. Additionally, each subject underwent a training session to ensure they understood the experimental task and how to properly use the probe.

At the beginning of training sessions, a virtual scale model of the probe was displayed, anchored at the center of the display and with its orientation mirroring that of the physical probe. A second virtual target probe was displayed in a similar fashion to serve as the orientation goal. Subjects were guided through four different levels of visual aids to align the virtual probe to the orientation goal and become accustomed to using the probe. The first visual aid level provided color cues on the goal to indicate alignment between the probe and the goal; the second level removed the color cues; the third level removed the virtual probe but restored the color cues; and the fourth removed both the virtual probe and color cues, displaying only the goal probe. Subjects were provided with feedback on the amount of error for each practice trial, and at least three practice trials of each visual aid level were required to be completed with an error of approximately 10° or less. Subjects were then shown examples of each stimulus condition and asked to orient the probe with the flow direction at the target marker while being given verbal feedback on their angular error with the target.

During the study, subjects were shown flow visualizations (as described the next section) and asked to estimate the direction of the flow through the cutting plane at a point indicated by a target marker (shown in Figure 4). Subjects indicated this by orienting the physical probe in front of them, near their line of sight with the display (so that there is minimal perspective distortion between the stimuli and the probe). When subjects were satisfied with the probe's orientation, they pressed a key to record the orientation and advance to the next trial. The angular error between the target vector and probe vector was recorded, along with elapsed decision time.

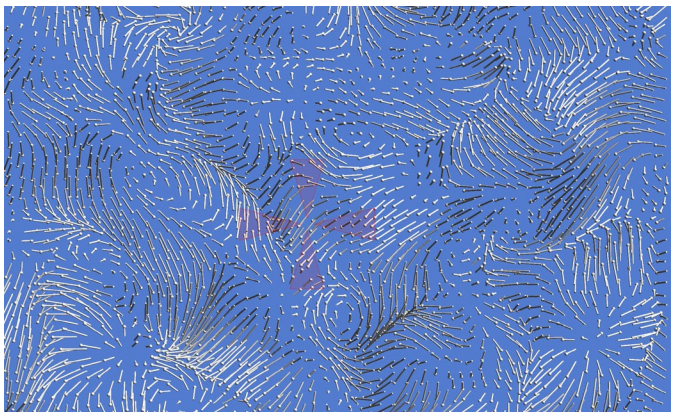

Fig. 4. Example screenshot, showing the target marker (red).

4 STIMULI

The experimental model is a fully-crossed 9x3 within-subjects randomized complete block design which evaluates three primary cutting plane parameters: nine different glyph conditions comprised of five different *glyph techniques* and three *diameter* values for the two 3D tube-based glyph techniques; and three *seeding densities* of these glyph conditions on the cutting plane.

Every subject saw each of the 27 rendering conditions a total of 10 times, resulting in 270 trials per subject. For each subject, the trials were presented in two randomized blocks, with each block containing five sequential replicates of the randomized conditions. The order of conditions was randomized per-block and per-subject to help control for ordering effects.

There does not seem to be a consensus on the best lighting style to use; Forsberg et al. [37] and Mallo et al. [41] suggest employing an additional headlight to further disambiguate lit geometry, but Penney et al. [39] found no performance difference for static scenes between ray-traced and standard OpenGL multi-lighting scenarios for depth perception tasks.

We used a single, directional light source, keeping lighting parameters consistent throughout all experimental conditions. The lighting direction was from above the right shoulder of the viewer at infinity ((-1, -1, -1), assuming right-handed coordinate system, xy-plane on the screen, and z-axis towards viewer). Subjects were made explicitly aware of the lighting direction during the training phase to help with their judgements.

Glyphs were displayed atop a light blue background to maintain an effective level of contrast for the stimuli. This background color was tuned during the pilot study; other colors were found to be too distracting or fatiguing, while white/grayscale backgrounds made it more difficult to use shading cues. A standard Blinn-Phong shading model was used to shade the spherical glyph heads and tube-based glyphs with the following lighting (L) and material (k) parameters: $L_a = 0.2$, $L_d = 1.0$, $L_s = 0.5$; $k_a = 0.5 * k_d$, $k_d = 1.0$, $k_s = 0.5$, $k_{shininess} = 10$. Though an orthographic projection of the stimuli could have been used, the stimuli were rendered using a perspective projection from a frustum modelled after the physical viewing conditions of the study to match reality as closely as possible.

Seeds were evenly distributed across the cutting planes, spaced on a regular grid based on the desired density value. Seeds were then slightly jittered by moving them randomly within ¼ of the spacing value before generating the glyph. This jittering was done as a precaution, because regular spacing can potentially induce meaningless patterns with some glyph techniques [1][12]. Furthermore, adding jitter is unlikely to negatively affect results; Laidlaw et al. [24] found no performance difference between regular and jittered grids for 2D flow glyphs.

Cutting planes displayed slices sampled from randomly-generated trivariate vector fields. These artificial vector fields were created by summing multiple random Gabor functions oriented along the three planes formed by each principle axis pair. After sampling, the slice is rendered using the current experimental condition and is displayed orthogonal to the subject's line of sight, filling the display screen.

A random location on the cutting plane is then selected as the target where subjects must estimate the direction of the flow. Because we did not employ head tracking, we mitigated any error due to perspective projection distortion by ensuring targets are selected from within the center half of the slice, where this error is much less pronounced.

4.1 Glyph Techniques

Five glyph techniques were selected from the literature for evaluation, as previously discussed in Section 2. Each of these approaches is representative of classes of common glyph designs, and each provides different sets of visual cues that support estimation of flow direction.

In all cases, a glyph is placed at each seed point, and extends in the direction of the flow according to the magnitude at that point. In our experimental dataset, target vectors magnitudes averaged 6.78 and ranged from 0.27 to 17.7 with a standard deviation of 2.56. For each glyph technique (except for shadowed lines, as explained in Section 4.1.3), one unit of magnitude is mapped to one millimeter of glyph length. Each glyph has a spherical head on its terminal end to disambiguate the overall direction.

4.1.1 Plain Lines

The plain lines technique serves as a control or baseline condition with which to compare the other techniques. As shown in Figure 5, the glyph is a plain white unlit line, which provides no depth cues except for the point at which it intersects its spherical head.

4.1.2 Illuminated Lines

The Illuminated Lines shading library [41] was used to augment the plain line technique by adding shading as an additional visual cue. The original method, developed by Zöckler et al. [29], was extended by determining the shading for the line through a model that approximates the total amount of light falling upon a cylinder with an infinitesimally-small diameter, which is then applied as the final color for the line. See Figure 6 for an example of this method.

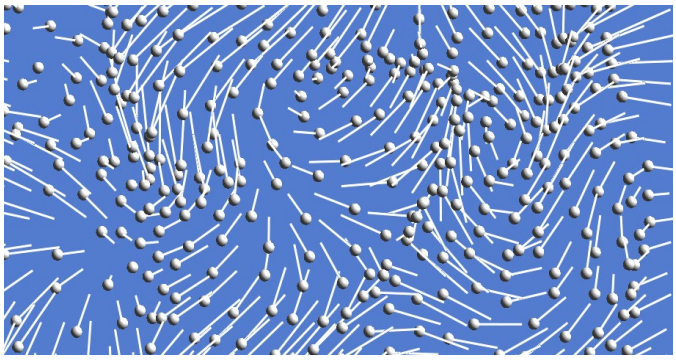

Fig. 5. Example of the "Plain Lines" technique.

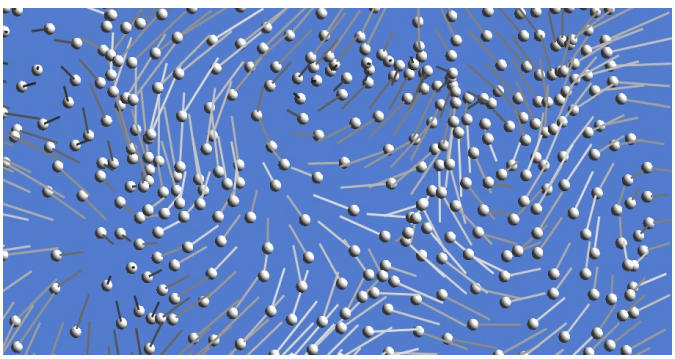

Fig. 6. Example of the "Illuminated Lines" technique.

4.1.3 Shadowed Lines

The "shadowed hedgehogs" technique developed by Klassen and Harrington [42], is a line-based technique that removes all shading and instead uses shadows to provide orientation and depth information, serving as a perfect specimen for studying cast shadows in relation to the other depth cues. The glyphs, shown in Figure 7, are still rendered in a perspective 3D projection but are colored black with no shading, and are anchored to the cutting plane by either their heads or tails, depending on whether the flow is directed into or out of the cutting plane. This modification facilitates the association of a glyph with its shadow; the original technique displaced the shadow plane behind the glyph plane, but we found that our modification yielded a better design when applied to a cutting plane.

Additionally, we found during pilot testing that the blue background made it very difficult to see the shadows. Since the glyphs themselves are entirely black, we decided to use a white background for conditions using this glyph technique to increase shadow contrast as much as possible. We believe that the advantage this modification offers outweighs the potential confounding effects of having a different background color from the other conditions.

To ensure regularity and eliminate glyph-glyph occlusions, grid jittering was not performed, and glyph lengths were normalized to ½ glyph spacing. Each 'hedgehog' glyph casts a light grey shadow onto the cutting plane based on the directional light source, giving a cue that, together with the glyph itself, theoretically provides all the information necessary to judge orientation.

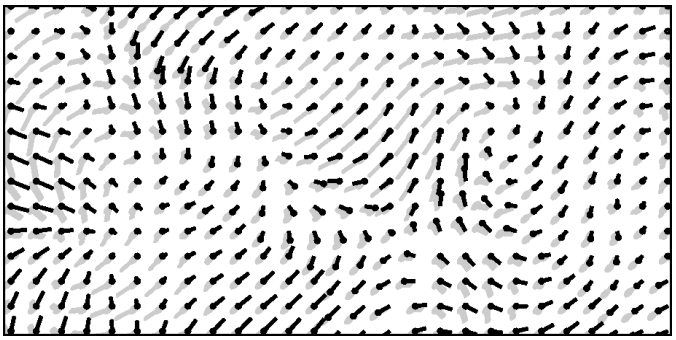

Fig. 7. Example of the "Shadowed Lines" technique.

4.1.4 Plain Tubes

Tube-based glyphs have the advantage of encoding multiple visual cues in their design, including shading, occlusion, and perspective. When one tube occludes another, we understand the occluded tube to be *behind* the occluding one (relative to ourselves). Perspective in this case results in foreshortening, where the projection of the tube diameter decreases with distance.

Another noteworthy theoretical benefit of tubes, which can be seen in Figure 8, is the appearance of the circular shape of the tail end. As a tube's orientation becomes more oblique with respect to the line of sight, the circular endcap deforms into an ellipse. These additional cues have the potential to increase the effectiveness of tube-based glyphs over plain lines.

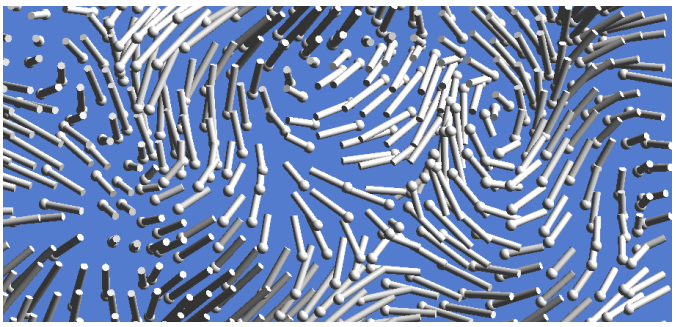

Fig. 8. Example of the "Plain Tubes" technique.

4.1.5 Ringed Tubes

Ringed tubes (pictured in Figure 9) are plain tubes with the addition of a regular ringed texture. Each of these individual rings help with perceiving orientation by reinforcing perspective cues in the same way as the singular circular tail end of a plain tube. However, the addition of this texture does increase visual noise, which has the potential to hinder orientation perception. The rings also serve as a redundant encoding of magnitude – longer glyphs will contain more rings.

Fig. 9. Example of the "Ringed Tubes" technique.

4.2 Seeding Density

The density of seeds on the cutting plane was also varied, to determine the optimal density for each technique and find points of diminishing returns. Too few seeds risks missing finer flow patterns. Too many seeds leads very quickly to problems with occlusion and overwhelming visual noise.

The three seeding densities evaluated in this experiment use intervals of 2, 3, and 4 seeds/cm, which correspond to 5mm, 3.33mm, and 2.5mm Cartesian grids, respectively. These conditions were determined from the pilot study to be adequate parameters for representing the usable ranges of possible seeding densities.

4.3 Glyph Diameter

For three-dimensional glyphs (i.e. the tube-based methods), an additional parameter of interest is glyph diameter. Thinner diameters make shading and circular-distortion orientation cues more difficult to discern, but allow for more densely-seeded cutting planes before occluding effects become an issue. On the other hand, thicker diameters have a higher chance of occluding one another at sparser seeding densities, but enhance the shading and orientation cues, making them easier to distinguish. This experiment tested tube glyph diameters of 0.5mm, 1mm, and 2mm, which were determined through pilot study evaluations in combination with the seeding densities.

5 Results

A total of 14 adult subjects participated in the study. Of these, 6 were female and 8 were male. Each subject was paid $27 for their participation, and each session lasted approximately 75 minutes: about 15 minutes for training and an average of 43 minutes viewing stimuli, the remaining 17 minutes representing between-condition and between-block breaks to help control for subject fatigue.

Trials where subjects took an inordinate amount of time to make a decision were filtered using Leys et al.'s approach [43] to finding outlier decision times. A conservative cutoff value of 26s over the mean time of 6.88s removed 2% of trials, leaving 3792 trials total.

It should be noted that F-tests for significant effects use the Kenward-Rogers approximation [44], which reduces bias from small sample sizes and responds well to removed outlier samples.

Because subjects' overall performance varied widely, we evenly divided the 14 subjects into two performance groups: one containing the top 7 performers and one containing the bottom 7 performers, based on their overall mean total angular error (28.9° and 36.6°, respectively). We found a highly significant main effect of group

membership ($F(1, 377.1) = 39.65$, $p < 0.0001$) on total angular error (described in the proceeding section); the following results are thus presented both for the entire subject pool (n=14), as well as split by each performance group (n=7) for cases where the split reveals more nuanced effects.

Additionally, the study data has been made publicly available for further analysis, and can be found at http://ccom.unh.edu/vislab/vis2016/hairy_slices_data.zip.

5.1 Analysis

First, we define how we calculate total angular error and its decomposition into depth error and weighted projection error. Given unit vectors $\hat{t}$ and $\hat{p}$ for the directions of the target and probe vectors, respectively, the total angular error θ is found using the formula:

$$\theta = \frac{180}{\pi} \cdot \cos^{-1}(\hat{t} \cdot \hat{p}) \quad (1)$$

Depth error is the absolute difference between the angle from the cutting plane to the target vector and the angle from the cutting plane to the probe vector. This depth error provides a measure of accuracy for depth perception. It is calculated as the difference in arc cosines of the z-component of the target and probe unit vectors:

$$\theta_D = \frac{180}{\pi} \cdot |\cos^{-1} \hat{t}_z - \cos^{-1} \hat{p}_z| \quad (2)$$

Projection error is the angular difference between target and probe vectors when projected onto the cutting plane. A weighting factor was used to correct for the deceptively large projection errors that can result from even small overall angular errors when target vectors are nearly parallel with the viewing direction. These parallel target vectors, which come straight at or away from viewers, received the lowest weight, while vectors orthogonal to the viewing direction (i.e. along the cutting plane) were assigned the highest weights. The formula for weighted projection errors is given as:

$$\theta_P = \frac{180}{\pi} \cdot \cos^{-1}\left(\frac{t_{xy} \cdot p_{xy}}{\|t_{xy}\| \cdot \|p_{xy}\|}\right) \cdot (1 - |t_z|) \quad (3)$$

Analysis of the data was performed using JMP statistical software in two stages. The first stage looked at the overall effects of the nine glyph conditions and three seeding densities, plus the possible interaction between these on total angular errors, decomposed angular errors, and decision time. Post-hoc analysis with Tukey's Honestly Significant Difference (HSD) test at the $p < 0.05$ confidence level was used to more conservatively group the glyph conditions and seeding densities.

The second analysis stage examined only the tube-based conditions for significant main effects of glyph technique, seeding density, and glyph thickness on total angular error, decomposed angular error, and decision time. Two-way interactions between these terms were also analysed, and a Student's t-test was used to compare the plain and ringed tube glyphs for any significant differences.

Before running the statistical analyses, the raw data were transformed using the Johnson S_L distribution function [45] to normalize the distributions of the variables in order to satisfy the prerequisites of the chosen analytical methods.

5.2 Total Angular Error

As shown in Figure 10, for total angular error, glyph condition was a highly significant factor, $F(8, 351.9) = 26.34$, $p < 0.0001$. The Tukey's HSD test split the techniques into five significantly different but overlapping ranks at the $p < 0.05$ confidence level: 2mm plain tubes came out on top, followed by the other tube-based conditions, except for 0.5mm ringed tubes, whose performance was not significantly different from the shadowed lines group. The two worst performing glyph conditions were illuminated lines and plain lines.

While the low-performance subject group demonstrates a stratification and overlap of glyph condition rankings similar to the overall dataset, the Tukey HSD analysis found only three distinct and completely separate groups within the high-performance group: all of the tube-based conditions in the top rank, followed by shadowed and illuminated lines, then plain lines.

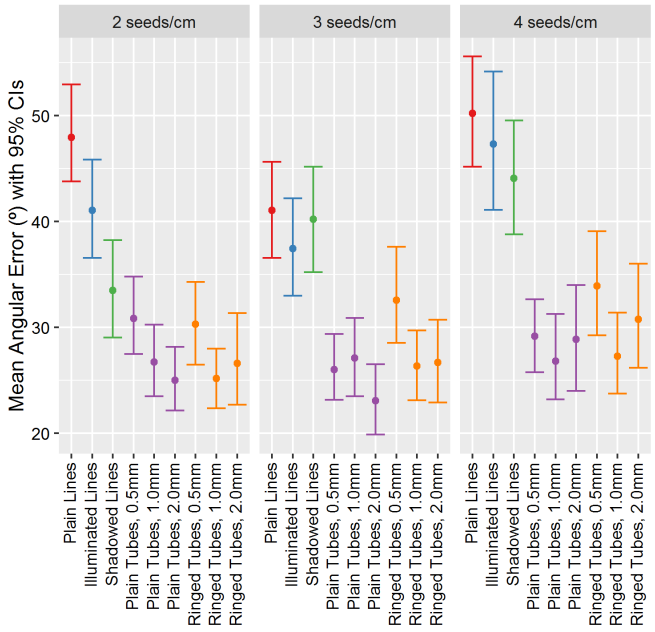

Fig. 10. Mean total angular error with bootstrapped 95% confidence intervals for each glyph condition and seeding density.

Overall, seeding density was a significant factor $F(2, 351.9) = 3.59$, $p = 0.0285$. The Tukey HSD analysis identified 3 seeds/cm as being significantly better than 4 seeds/cm at the $p < 0.05$ confidence level, but no significant differences between the 2 seeds/cm level.

There was no significant interaction found between glyph condition and density for the overall subject pool, nor for the individual performance groups.

For tube based glyphs, tube diameter had a highly significant effect ($F(2, 239) = 6.85$, $p = 0.0013$) on total angular error, and the Tukey HSD test found that 1 mm and 2 mm diameters are significantly better than 0.5 mm diameters at the $p < 0.05$ confidence level. Interestingly, breaking this result down by performance group reveals that the middle-sized 1 mm tube diameter was only significantly better than the 0.5 mm diameter for high-performing subjects; i.e. low-performing subjects did not perform as well with the 1 mm tube diameter conditions. There was no significant main effect of seeding density nor glyph technique, and none of the interaction terms reached significance.

There was some concern that the experimental design may provide the two tube-based glyph techniques with an advantage by being seen 3 times as frequently as the other line-based glyph techniques, due to the three different diameter conditions that only apply to tube-based techniques. To assess this potential bias, the first 15 trials from each glyph technique (regardless of tube diameter) for each subject were extracted to enable a balanced and unbiased analysis. An ANOVA of the total angular error on this data subset revealed a highly significant effect of glyph condition ($F(4, 194) = 12.10$, $p < 0.0001$) but not seeding density. The glyph techniques were grouped into four overlapping but significantly different groups at the $p < 0.05$ confidence level: plain tubes first, followed by ringed tubes, shadowed lines, illuminated lines, and plain lines in the worst group. As these rankings follow the same pattern as those from the larger dataset, we can conclude that any biasing effect introduced by the relative frequency of tube-based techniques is overpowered by the larger effects of technique difference.

5.3 Depth Error

Depth errors for the different glyph conditions and seeding densities are shown in Figure 11. Again, there was a highly significant effect ($F(8, 350.2) = 31.71$, $p < 0.0001$) of glyph technique, with performance of the different techniques being almost identical to the observations of total angular error in Section 5.2. The Tukey HSD test

grouped the conditions into four main groups at the $p < 0.05$ confidence level: 2 mm tubes are better than 0.5 mm tubes, but 1 mm tubes are not significantly different from either; the next group contains shadowed lines, and illuminated lines lies between that group and the worst group which contains only plain lines.

Seeding density also had a significant ($F(2, 350.2) = 3.66$, $p = 0.0267$) effect on depth errors, and these were grouped in the same manner as they were for total angular error in Section 5.2 by the Tukey HSD test at a $p < 0.05$ confidence level.

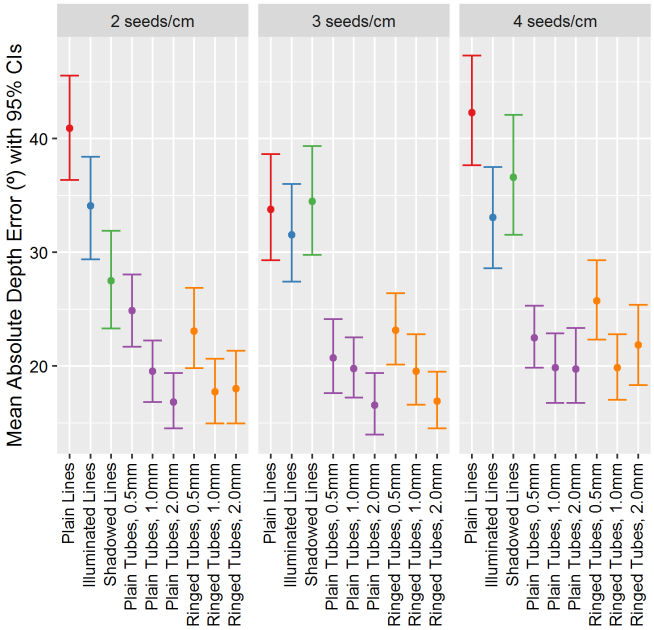

Fig. 11. Absolute depth error with bootstrapped 95% confidence intervals for each glyph technique and seeding density.

For tube based glyphs, again only the diameter had a significant effect ($F(2, 237.5) = 13.99$, $p < 0.0001$) on depth error. The diameter groupings found by a Tukey HSD analysis at the $p < 0.05$ confidence level are the same as those found for total angular error in section 5.2. An interesting finding is that, while the high-performance subject group showed the same significant effects and groupings as the combined data, the low-performance group had an additional significant main effect of seeding density, $F(2, 111.8) = 3.47$, $p = 0.0344$. A Tukey HSD analysis found that 3 seeds/cm are significantly better than 4 seeds/cm at the $p < 0.05$ confidence level, just like what was found for total angular error.

5.4 Projection Error

As shown in Figure 12, for projection errors, the performance differences between different glyph conditions and seeding densities is much less apparent. Considering all subjects, glyph technique had a significant effect ($F(8, 350.9) = 2.56$, $p = 0.0101$), but only in the case of 0.5 mm plain tubes performing better than shadowed lines. Interestingly, when broken down by performance group, this advantage of 0.5 mm plain tubes over shadowed lines was only observed in high-performing subjects; low-performing subjects showed no significant difference between any glyph techniques.

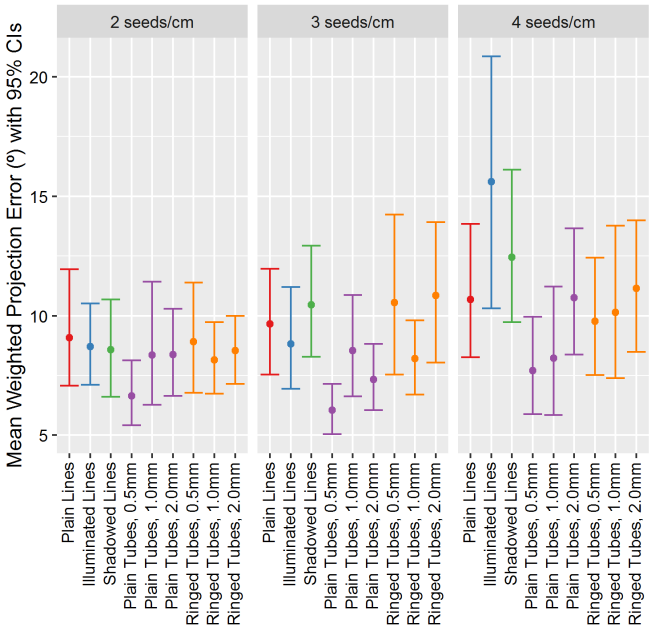

Fig. 12. Weighted projection error with 95% confidence intervals for each glyph technique and seeding density.

Seeding density had no significant main effect on projection error, nor did the interaction between seeding density and glyph.

For tube-based glyphs, neither tube diameter nor seeding density had a significant effect on projection error, but glyph technique was highly significant ($F(1, 238) = 7.27$, $p = 0.0075$). The Student's t-test found plain tubes to be significantly better than ringed tubes at the $p < 0.05$ confidence level.

5.5 Decision Times

The analysis of the data did not show any significant main effects or interactions on decision times for either the overall dataset or within the two performance groups.

5.6 Feedback

A post-study questionnaire was given to each subject to collect impressions about the different glyph techniques. Subjects were asked to rate each technique on a scale from one (worst) to five (best) in response to four questions.

When asked whether the glyph technique was intuitive and easy to understand, subjects rated plain tubes highest ($\bar{x} = 4.1$, $SD = 0.5$), followed by ringed tubes ($\bar{x} = 3.8$, $SD = 0.8$), illuminated lines ($\bar{x} = 3.4$, $SD = 0.5$), plain lines ($\bar{x} = 2.4$, $SD = 0.8$), and shadowed lines ($\bar{x} = 2.3$, $SD = 1.2$).

When asked whether the subject thought they got better and faster using a glyph technique over the course of the study, subjects rated plain tubes highest ($\bar{x} = 4.2$, $SD = 0.4$), followed by ringed tubes ($\bar{x} = 4.0$, $SD = 0.6$), illuminated lines ($\bar{x} = 3.9$, $SD = 0.7$), plain lines ($\bar{x} = 3.6$, $SD = 0.6$), and shadowed lines ($\bar{x} = 3.1$, $SD = 1.3$).

When asked whether the glyph technique was aesthetically pleasing and enjoyable to look at, subjects rated plain tubes highest ($\bar{x} = 3.8$, $SD = 1.0$), followed by ringed tubes ($\bar{x} = 3.6$, $SD = 1.1$), illuminated lines ($\bar{x} = 3.4$, $SD = 0.9$), plain lines ($\bar{x} = 3.0$, $SD = 1.0$), and shadowed lines ($\bar{x} = 2.4$, $SD = 1.2$).

When asked whether it took a long time to make a decision using the glyph technique, subjects rated plain tubes and ringed tubes fastest ($\bar{x} = 2.6$, $SD = 0.9$; $\bar{x} = 2.6$, $SD = 1.1$; respectively), illuminated lines ($\bar{x} = 3.0$, $SD = 0.6$), plain lines ($\bar{x} = 3.4$, $SD = 0.7$), and shadowed lines ($\bar{x} = 3.9$, $SD = 1.4$) slowest.

6 Discussion

Overall, the results seem to fit the expected pattern. Tube-based glyph techniques proved to be significantly better for orientation perception than the illuminated lines and shadowed lines techniques, which were better than plain lines. This makes sense, as the tubes provide more visual cues for orientation than the other glyph techniques, and are easier to distinguish from one another in denser seeding conditions than line-based methods. In fact, tube-based techniques exhibited resistance to the performance decrease that other techniques were subject to as seeding density increased, evidenced by the significant interaction between glyph technique and seeding density within the high-performing split group.

Further examination of the high-performing split group reveals a clear hierarchy of glyph techniques, ordered by available visual cues. The lack of significant effects on weighted projection errors supports this grouping, since no depth information should be needed to accurately determine the projection of a vector onto a viewing plane.

6.1 Texture Cue Performance

Texture cues did not appear to play a significant role in perceiving orientation, as ringed tubes did not perform any differently than plain tubes. One explanation for this may be that the addition of texture introduces extra visual cognitive load instead of helpful cues, hurting performance instead of helping it. This merits further exploration in the role of textures that directly encode information, as in Stoll et al.'s texture arrows [30] or Fuhrmann and Gröller's animated dashtubes [27] to indicate flow direction.

The addition of the ringed texture to the tubes also may have contributed to glyphs visually fusing with one another. Since the ring color contrasts with the lighter tube color, it may diminish the ability of the visual system to use the subtler shading cues and high-contrast contour edges to disambiguate individual glyphs. For helping to distinguish occluding 3D elements from one another, the halo technique has been used extensively [10][31][46]. This modification could provide the necessary visual separation between glyphs to allow textures to provide the strong additive benefits that they have exhibited in other studies.

6.2 Cast Shadows Cue Performance

The cast shadows cue definitely gave the shadowed lines technique an advantage over the other line-based techniques, but it was also highly sensitive to seeding density. At the sparsest density (5-mm spacing), the performance of the shadowed lines technique approached that of the tube-based techniques. This is noteworthy, as the tube-based techniques utilize form-revealing shading that directly visualizes an orientation, whereas the shadowed lines technique requires the integration of two individual components to understand the whole glyph. These results suggest that cast shadows may be a strong cue for perceiving the orientation of objects lacking strong shading or for partially occluded objects whose shading is obscured.

However, user feedback was overwhelmingly negative for the shadowed lines technique. Although it achieved respectable performance results when compared to the other line-based techniques, subjects rated shadowed lines as the most negative in every category: aesthetics, ease of interpretation, speed of decision, and how well they think they performed using the technique. This lesson underscores the importance of real-world evaluations to strike a balance between what works in the lab and what works in practice.

Nonetheless, the relative success of the shadowed lines technique compared to other line-based techniques hints at the potential for shadows to be a useful additive depth cue to be used alongside sparsely-seeded 3D glyphs.

6.3 Future Work

An additional avenue for future study is the effect of the cutting plane orientation on the perception of these glyphs. This study evaluated only cutting planes that were orthogonal to the viewing direction. There is evidence that orientation perception changes with viewing angles for surface contours [47], which may also be the case in this context. However, more oblique viewing angles can increase occlusion and visual clutter. These issues could be addressed with additional visual aids such as glyph halos and depth cueing.

Another option with obvious performance implications would be to add stereoscopic viewing or kinetic depth via cutting plane interaction, which should provide stronger depth cues that predominate the others, and result in a better environment for viewing oblique cutting planes.

An examination of different tube designs in the context of stereopsis and kinetic depth may provide further insights. It is likely that, using a high-resolution stereoscopic display, fine texturing and shading will take advantage of the superacuity of binocular vision to offer stronger depth cues than would otherwise be possible with monoscopic renderings. An expansion of this study could also evaluate other glyph techniques beyond ringed textures and three-dimensional geometric designs, especially those that incorporate an intuitive directional component into them such as cones.

7 Conclusions

3D vector field visualization has been widely researched, and many successful designs have been identified. Despite widespread use of these visualizations in the sciences, there have been few empirical studies of these designs to ascertain the underlying perceptual cues that make them effective.

This paper directly addressed this lack of objective, quantitative formal studies that explore the perceptual effectiveness of three-dimensional flow visualizations by conducting an experiment to investigate the monoscopic visual cues integral to the use of 3D glyphs on cutting planes.

The results of the experiment confirmed the hypotheses that increasing the dimensionality of lines into tubular structures enhances their ability to convey orientation through shading, and that increasing their diameter intensifies this effect. It also confirmed that adding shadows to lines increases depth perception. Interestingly, while it was hypothesized that adding a ringed texture to tubes would increase depth and orientation perception, no significant effect was found, possibly due to increased visual noise.

From these results, a number of guidelines can be drawn for designing effective glyph-based 3D vector field visualization:

- Use tubes instead of lines for better orientation perception. Their thicker 3D form presents stronger shape-from-shading cues, a clear advantage over line-based techniques.
- Avoid overly dense seeding of glyphs on cutting planes. Tightly packed glyphs can visually fuse together. Tube-based glyphs are less sensitive to fusion issues. However, occlusion is an issue with any glyph type.
- Use caution when applying texture to glyphs. Unless the texture adds specific information, the additional visual noise can be detrimental.
- Provide shadows where possible. They provide redundant orientation cues, as long as they can be unambiguously associated with the objects casting them.

Of course, cues that are objectively helpful in theory are not always practical. User feedback on visualizations is just as important as a grounding in perceptual theory; a visualization is ultimately worthless if end-users find it obnoxious or disagreeable. This was seen in this study with the good performance, but terrible user rating, of shadowed lines.

Acknowledgments

This work was supported by NOAA Grants #NA10NOS4000073 and #NA15NOS4000200.

References

[1] R. Borgo, J. Kehrer, D.H. Chung, E. Maguire, R.S. Laramee, H. Hauser, M. Ward, M. Chen, "Glyph-based visualization: Foundations, design

guidelines, techniques and applications", Eurographics State of the Art Reports, pp. 39-63, 2013.
[2] C. Johnson, R. Moorhead, T. Munzner, H. Pfister, P. Rheingans, T.S. Yoo, "NIH/NSF visualization research challenges report" IEEE Computer Graphics and Applications, vol. 26, no. 2, pp 20-24, 2006.
[3] T. Munzner, "Visualization Analysis and Design", CRC Press, 2014.
[4] MATLAB, The MathWorks Inc., http://www.mathworks.com
[5] E. Boring, A. Pang, "Directional flow visualization of vector fields", Proc. IEEE Visualization '96, pp. 389-392, 1996.
[6] N. Elmqvist, P. Tsigas, "A taxonomy of 3D occlusion management for visualization", IEEE TVCG, vol. 14, no. 5, pp. 1095-1109, 2008.
[7] R.S. Laramee, D. Weiskopf, J. Schneider, H. Hauser, "Investigating swirl and tumble flow with a comparison of visualization techniques", Proc. IEEE Visualization '04, pp. 51-58, 2004.
[8] T. McLoughlin, R. S. Laramee, R. Peikert, F. H. Post, M. Chen, "Over Two Decades of Integration-Based, Geometric Flow Visualization." In Computer Graphics Forum, vol. 29, no. 6, pp. 1807-1829, Sept 2010.
[9] B. Cabral, L.C. Leedom, "Imaging vector fields using line integral convolution", Proc. ACM SIGGRAPH '93, pp. 263-270, 1993.
[10] V. Interrante, C. Grosch, "Visualizing 3D flow", IEEE Computer Graphics and Applications, vol. 18, no. 4, pp. 49-53, 1998.
[11] F.H. Post, B. Vrolijk, H. Hauser, R.S. Laramee, H. Doleisch, "Feature extraction and visualization of flow fields", Eurographics '02 State-of-the-Art Reports, pp. 69-100, 2002.
[12] C. Ware, "Information visualization: perception for design", Elsevier, 2012.
[13] G.V. Bancroft, F.J. Merritt, T.C. Plessel, P.G. Kelaita, R. K. McCabe, A. Globu, "FAST: A multi-processing environment for visualization of computational fluid dynamics", Proc. IEEE Visualization '90, pp. 14–27, 1990.
[14] M. Giles, R. Haimes, "Advanced interactive visualization for CFD", Computing Systems in Engineering, vol. 1, no.1, pp.51-62, 1990.
[15] C. Upson, T. Faulhaber Jr., D. Kamins, D. Laidlaw, D. Schlegel, J. Vroom, R. Gurwitz, A. van Dam, "The application visualization system: A computational environment for scientific visualization", IEEE Computer Graphics and Applications, vol. 9, no. 4, pp. 30–42, 1989.
[16] VTK, The Visualization Toolkit, http://www.vtk.org/
[17] PowerFLOW, Exa Corporation, http://exa.com/product/powerflow
[18] J.R. Osborn, A.M. Agogino, "An interface for interactive spatial reasoning and visualization", Proc. ACM SIGCHI '92, pp. 75-82, 1992.
[19] J. Diepstraten, D. Weiskopf, T. Ertl, "Interactive Cutaway Illustrations", Computer Graphics Forum, vol. 22, no. 3, pp. 523–532, 2003.
[20] M. Schulz, F. Reck, W. Bertelheimer, T. Ertl, "Interactive visualization of fluid dynamics simulations in locally refined Cartesian grids", Proc IEEE Visualization '99, pp. 413-553, 1999.
[21] T. Meyer, A. Globus, "Direct manipulation of isosurfaces and cutting planes in virtual environments", Technical Report CS-93-54, Department of Computer Science, Brown University, 1993.
[22] K. Hinckley, R. Pausch, J.C. Goble, N.F. Kassell, "Passive real-world interface props for neurosurgical visualization", Proc. ACM SIGCHI '94, pp. 452-458, 1994.
[23] D.L. Modiano, "Visualization of three dimensional CFD results", CFDL Technical Report 89-4, MIT, 1987.
[24] D.H. Laidlaw, R.M. Kirby, C.D. Jackson, J.S. Davidson, T.S. Miller, M. Da Silva, W.H. Warren, M.J. Tarr, "Comparing 2D vector field visualization methods: A user study", IEEE TVCG, vol. 11, no. 1, pp. 59-70, 2005.
[25] Z. Liu, S. Cai, J.E. Swan, R.J. Moorhead, J.P. Martin, T.J. Jankun-Kelly, "A 2D flow visualization user study using explicit flow synthesis and implicit task design", IEEE TVCG, vol. 18, no. 5, pp. 783-796, 2012.
[26] O. Konrad-Verse, A. Littmann, B. Preim, "Virtual Resection with a Deformable Cutting Plane", Proc. SimVis '04, pp. 203-214, 2004.
[27] A. Fuhrmann, E. Gröller, "Real-time techniques for 3D flow visualization", Proc. IEEE Visualization '98, pp. 305-312, 1998.
[28] C.M. Wittenbrink, A. Pang, S.K. Lodha, "Glyphs for Visualizing Uncertainty in Vector Fields", IEEE TVCG, vol. 2, no. 3, pp. 266-279, 1996.
[29] M. Zöckler, D. Stalling, H.C. Hege, "Interactive visualization of 3D-vector fields using illuminated stream lines", Proc. IEEE Visualization '96, pp. 107-113, 1996.
[30] C. Stoll, S. Gumhold, H.P. Seidel, "Visualization with stylized line primitives", Proc. IEEE Visualization '05, pp. 695-702, 2005.
[31] A. Wenger, D.F. Keefe, S. Zhang, D.H. Laidlaw, "Interactive volume rendering of thin thread structures within multivalued scientific data sets", IEEE TVCG, vol. 10, no. 6, pp. 664-672, 2004.
[32] D. Darmofal, R. Haimes, "Visualization of 3-d vector fields: Variations on a stream", AIAA 30th Aerospace Science Meeting and Exhibit, Jan 1992.
[33] A.E. Lie, J. Kehrer, H. Hauser, "Critical design and realization aspects of glyph-based 3D data visualization", Proc. ACM SCCG '09, pp. 19-26, 2009.
[34] C.K. Chen, S. Yan, H. Yu, N. Max, K.L. Ma, "An illustrative visualization framework for 3d vector fields", Computer Graphics Forum, vol. 30, no. 7, pp. 1941-1951, 2011.
[35] A. Brambilla, R. Carnecky, R. Peikert, I. Viola, H. Hauser, "Illustrative flow visualization: State of the art, trends and challenges", Visibility-oriented Visualization Design for Flow Illustration, 2012.
[36] C. Ware, "3d contour perception for flow visualization", Proc. ACM APGV '06, pp. 101–106, 2006.
[37] A.S. Forsberg, J. Chen, D.H. Laidlaw, "Comparing 3d vector field visualization methods: A user study", IEEE TVCG, vol. 15, no. 6, pp. 1219–1226, 2009.
[38] J. Chen, H. Cai, A.P. Auchus, D.H. Laidlaw, "Effects of stereo and screen size on the legibility of three-dimensional streamtube visualization", IEEE TVCG, vol. 18, no. 12, pp. 2130-2139, 2012.
[39] D. Penney, J. Chen, D.H. Laidlaw, "Effects of illumination, texture, and motion on task performance in 3D tensor-field streamtube visualizations", Proc. IEEE PacificVis '12, pp. 97-104, 2012.
[40] F. Campbell, D. Green, "Optical and retinal factors affecting visual resolution", The Journal of Physiology, vol. 181, no. 3 p. 576-593, 1965.
[41] O. Mallo, R. Peikert, C. Sigg, F. Sadlo, "Illuminated lines revisited", Proc. IEEE Visualization '05, pp 19-26, 2005.
[42] R.V. Klassen, S.J. Harrington, "Shadowed hedgehogs: A technique for visualizing 2d slices of 3d vector fields", Proc IEEE Visualization '91, pp. 148–153, 1991.
[43] C. Leys, C. Ley, O. Klein, P. Bernard, L. Licata, "Detecting outliers: Do not use standard deviation around the mean, use absolute deviation around the median", Journal of Experimental Social Psychology, vol. 49, no. 4, pp. 764 – 766, 2013.
[44] M.G. Kenward, J.H. Roger, "Small sample inference for fixed effects from restricted maximum likelihood", Biometrics, vol. 53, no. 3, pp. 983–997, 1997.
[45] J. F. Slifker, S. S. Shapiro. "The Johnson System: Selection and Parameter Estimation." Technometrics, vol. 22, no. 2, pp. 239-246, 1980.
[46] M.H. Everts, H. Bekker, J.B. Roerdink, T. Isenberg, "Depth-dependent halos: Illustrative rendering of dense line data", IEEE TVCG, vol. 15, no. 6, pp. 1299-1306, 2009.
[47] G. Sweet, C. Ware, "View direction, surface orientation and texture orientation for perception of surface shape", Proc. Graphics Interface, pp. 97–106, 2004.